Chemical Engineering Science 65 (2010) 3798–3807

Contents lists available at ScienceDirect

Chemical Engineering Science

journal homepage: www.elsevier.com/locate/ces

Modelling PCC flocculation by bridging mechanism using population balances: Effect of polymer characteristics on flocculation

E. Antunes [a], F.A.P. Garcia [b], P. Ferreira [a], A. Blanco [c], C. Negro [c], M.G. Rasteiro [a,*]

[a] Research Centre for Chemical Processes Engineering and Forest Products, Chemical Engineering Department, Coimbra University, Pólo II, Pinhal de Marrocos, 3030-790 Coimbra, Portugal
[b] Chemical Engineering Department, Coimbra University, Pólo II, Pinhal de Marrocos, 3030-790 Coimbra, Portugal
[c] Chemical Engineering Department, Faculty of Chemistry, Complutense University, 28040 Madrid, Spain

ARTICLE INFO

Article history:
Received 19 October 2009
Received in revised form
13 January 2010
Accepted 13 March 2010
Available online 19 March 2010

Keywords:
Population balance
Flocculation dynamics
Branched polyelectrolytes
Flocs characteristics
Flocs restructuring
Papermaking

ABSTRACT

A population balance model for flocculation of PCC particles with polyelectrolytes of very high molecular weight, medium charge density and different degree of branching is presented. The model considers simultaneously aggregation, breakage and flocs restructuring to describe the PCC flocculation by bridging mechanism. The maximum collision efficiency factor, a parameter related with the fragmentation rate and a time constant for flocs restructuring have been taken as fitting parameters. These fitting parameters are optimized to get the best fit between experimental data obtained by LDS in a previous study and the modelled results. The optimized parameters were correlated with flocculant concentration, flocs structure and polymer branching. The correlations obtained show well the effects of flocculant concentration, flocs structure and polymer structure on the flocculation kinetics and flocs restructuring which are translated in the model parameters. Moreover, the flocs break up due to polymer degradation was introduced in the model by decreasing, with time, the maximum collision efficiency factor. It was shown that this effect can be neglected since the improvement in the results is too small relatively to the high increase of the computational time required to perform the simulation.

1. Introduction

Characterisation and control of aggregates' properties are of great importance since size, shape and structure of the flocs are related with both the process efficiency and the final product quality (Yukselen and Gregory, 2004). This is the case, for example, of the papermaking process where the flocs structure and size depend namely on the flocculant concentration, polymer characteristics and mixing rate (Norell et al., 1999). Hence, it is necessary to monitor and manipulate adequately these parameters to control flocs size and structure during the formation of the paper sheet.

Consequently, to understand, predict and control the aggregation process, quantitative models with capabilities to describe flocculation under various processing conditions need to be developed. The common modelling approach is based on population balance equations (PBE) (Thomas et al., 1999; Biggs et al., 2000; Liao et al., 2005; Heath et al., 2006).

The mathematical modelling of flocculation usually makes use of the classic Smoluchowski (1917) approach that describes the rate of irreversible aggregation. However, Smoluchowski made a number of simplifying assumptions to solve the model. He assumed that every collision is successful ($\alpha_{ij}=1$), the particles are of same size and both particles and aggregates are spherical in shape. In addition, binary collision between particles occurs due to laminar fluid motion and no flocs breakage is considered (Thomas et al., 1999). Thus, the analytical solution of this classical approach is significantly constrained by these assumptions and deviates from most real systems.

In this way, many authors proposed modifications to this equation and considerable progress has been made in using numerical techniques to model the growth of particles by aggregation (Thomas et al., 1999). More recently, the effects of turbulent shear rate, flocculant dosage, primary particle size and solid fraction have been incorporated into PBEs that now account simultaneously for aggregation and breakage (Heath et al., 2006). As stated by Thomas et al. (1999), the knowledge of the fractal dimension is useful to make flocculation modelling more applicable to real systems. Therefore, some authors have introduced the fractal dimension into PBEs to model the shear-induced flocculation of porous aggregates (Serra and Casamitjana, 1998; Flesch et al., 1999). However, these developments have usually been attempted by assuming a constant structure for all flocs during the process. Selomulya et al. (2003) have shown that flocs

* Corresponding author. Tel.: +351 239798700; fax: +351 239798703.
E-mail address: mgr@eq.uc.pt (M.G. Rasteiro).

0009-2509/$ - see front matter © 2010 Elsevier Ltd. All rights reserved.
doi:10.1016/j.ces.2010.03.020

structure changes considerably during flocculation. The flocs restructuring was incorporated into the PBEs by the fractal dimension, referred as the scattering exponent (Liao et al., 2005), which varies during flocculation time.

Moreover, since, based on experimental observations, the collision efficiency decreases as the aggregate size increases, Kusters et al. (1997) proposed a model where the collision efficiency decreased exponentially with increasing dimensionless floc size (aggregate radius/aggregate permeability). Furthermore, the collision efficiency factor not only depends on the flocs size but also on the flocculant characteristics. Swerin et al. (1996) have considered that the flocculation efficiency factor is proportional to the product of the fraction of the surface covered with adsorbed polymer on one particle and the non-covered fraction on the second particle. When the flocculant acts by the bridging mechanism, the layer thickness affects the collision efficiency. Hence, the collision efficiency factor is described by the bridging action and by the layer expansion that enhances collisions.

Heath and Koh (2003) and Heath et al. (2006) have proposed another way to introduce the decrease in the flocs size during flocculation, into the model. They considered that the decrease in the flocs size is due to polymer degradation as a consequence of flocs break up. In the first study (2003), this breakage irreversibility was introduced into the model by making the particle collision efficiency term decrease during flocculation time. In the second study (2006), the polymer degradation was incorporated in the breakage kernel.

In previous papers (Rasteiro et al., 2008a,b; Antunes et al., 2008), it was shown that flocculation of precipitated calcium carbonate (PCC) induced by cationic polyacrylamides (C-PAM) of very high molecular weight and medium charge density occurs by the bridging mechanism. As a result, the flocculation kinetic curves exhibit a maximum in the flocs size in the early instants of flocculation and, thereafter, the polymer undergoes reconformation. During this reconformation stage, restructuring of flocs occurs due to the polymer reconformation at the particle surface and flocs size decrease until reaching a steady state (Antunes et al., 2008). It was also demonstrated that flocculation kinetics and flocs structure (described by the fractal coefficient) depend on the flocculant concentration and structure (number of branches).

The aim of this study is to implement a population balance model that is able to describe the flocculation process of PCC particles induced by the bridging mechanism. Additionally, the model parameters will be correlated with the polymer characteristics (concentration and branching) in order to obtain a model that can predict the aggregates' characteristics (size and structure) or the operating conditions which produce aggregates with the characteristics required for a predefined task.

2. Model description

2.1. Population balance model

The discretized population balance equation proposed by Hounslow et al. (1988) and Spicer and Pratsinis (1996) has been widely used to describe flocculation with aggregation and breakage terms. The particle size interval was discretized by doubling the particle or floc volume (v_i) after each interval ($v_{i+1}=2v_i$), Eq. (1) being obtained.

$$\frac{dN_i}{dt}=\sum_{j=1}^{i-2}2^{j-i+1}\alpha_{i-1,j}\beta_{i-1,j}N_{i-1}N_j+\frac{1}{2}\alpha_{i-1,i-1}\beta_{i-1,i-1}N_{i-1}^2 -N_i\sum_{j=1}^{i-1}2^{j-i}\alpha_{i,j}\beta_{i,j}N_j-N_i\sum_{j=i}^{\infty}\alpha_{i,j}\beta_{i,j}N_j-S_iN_i+\sum_{j=i}^{\infty}\Gamma_{i,j}S_jN_j \quad (1)$$

N_i is the number concentration of flocs containing 2^{i-1} particles (#/cm^3). In this case, N_1 is the number concentration of primary particles. The first two terms of Eq. (1) describe the formation of flocs in the ith interval from the collisions of flocs from smaller size ranges. The third and fourth terms represent the loss of flocs in the ith interval by the aggregation of flocs from range i with those from other size intervals. The fifth term accounts for the loss of flocs in the ith interval through fragmentation, and the last term denotes the gain of flocs in class i by fragmentation of larger flocs. The parameters $\alpha_{i,j}$ and $\beta_{i,j}$ are the collision efficiency and the collision frequency, respectively, between flocs in the i and j intervals. The parameter S_i is the fragmentation rate of flocs in the i interval, whereas $\Gamma_{i,j}$ is the breakage distribution function for the break-up of flocs in interval j, which generates fragments of sizes that fall in the ith interval.

2.2. Collision efficiency

The presence of short-range forces such as electrostatic forces and of hydrodynamic interactions between particles can reduce the probability of attachment of two colliding particles, i.e., a collision between two particles could be unsuccessful and thus, the collision efficiency should be lower than unity (Thomas et al., 1999). In the case of the classical approach proposed by Smoluchowski, the collision efficiency is equal to unity because the model, called in this case rectilinear model, did not take into account hydrodynamic retardation and effects of colloidal interactions. The curvilinear models have been an alternative to the classical approach and were presented by several authors (Thomas et al., 1999). Adler (1981b) was the first to propose a model accounting for colloidal and hydrodynamic interactions. He demonstrated that collision frequency is higher when the colliding particles were of same size. Moreover, Han and Lawler (1992) developed numerical expressions to convert the rectilinear approach to a curvilinear model. These numerical expressions are functions of the size ratio of the colliding particles and of the ratio of the hydrodynamic interactions and attraction forces. The inclusion of the hydrodynamic interactions and attraction forces leads to a reduction of the flocculation rate and of the orthokinetic flocculation (Thomas et al., 1999). However, these models ignore that aggregates are porous. One way is to calculate the flow and associated drag on a porous sphere (Wu and Lee, 1998). Another model was developed by Kusters et al. (1991), using the trajectory analysis of Adler (1981a), to calculate the collision efficiency between porous aggregates. The collision efficiency calculated with the obtained semi-empirical equation decreased exponentially with the increasing dimensionless flocs size defined as the radius of the aggregate over its permeability. In this manner, the collision efficiency approached zero when the size ratio between flocs is lower than 0.1 and thus, the probability of attachment for larger and/or porous flocs is reduced. In this study, the model developed by Kusters et al. (1997) and described by Eq. (2) was introduced in the model based on Eq. (1) to take into account the effect of particles' size on the collision efficiency factor.

$$\alpha_{ij}=\left[\frac{\exp\left(-x\left(1-\frac{i}{j}\right)^2\right)}{(i\times j)^y}\right]\times\alpha_{\max} \quad (2)$$

i and j indicate the classes where colliding aggregates are located, $\alpha_{\max}$ is the upper limit of α_{ij} ($0\le\alpha_{\max}\le 1$) and x and y are fitting parameters. In this study, we have considered $x=y=0.1$ as in the work of Selomulya et al. (2003) and Soos et al. (2006). Selomulya et al. (2003) have shown that smaller values of x and y result in faster growth of the aggregates. The maximum collision

efficiency value (α_{max}) is an adjustable parameter as in the work of Soos et al. (2006).

2.3. Collision frequency

Assuming that the particles are fully destabilized, that the collisions due to settling are negligible (considering that $\rho_{water} \approx \rho_{particle}$, (Swift and Friedlander, 1964)) and that the mechanisms are independent of each other, the collision frequency between two particles is the result of the collision frequency due to Brownian motion and the collision frequency due to orthokinetic aggregation as described in equation below.

$$\beta_{ij} = \beta_{perikinetic} + \beta_{orthokinetic} \tag{3}$$

The collision frequency for Brownian motion is given by Eq. (4) (Smoluchowski, 1917) where k_B is the Boltzmann constant, T is the absolute temperature and μ is the viscosity of the fluid.

$$\beta_{ij,perikinetic} = \left(\frac{2k_BT}{3\mu}\right)\frac{(R_{ci}+R_{cj})^2}{R_{ci}R_{cj}} \tag{4}$$

The collision frequency for orthokinetic aggregation in isotropic turbulence is given by Eq. (5) (Saffman and Turner, 1956) where ε is the average energy dissipation rate and ν is the kinematic viscosity of the fluid.

$$\beta_{ij,orthokinetic} = 1.294\left(\frac{\varepsilon}{\nu}\right)^{1/2}(R_{ci}+R_{cj})^3 \tag{5}$$

In Eqs. (4) and (5), R_c is the effective capture radius and, for fractal aggregates, it can be calculated from Eq. (6) (Saffman and Turner, 1956) where r_0 is the primary particle radius, N is the number of primary particles in aggregate, k_c is a constant close to unity and d_F is the mass fractal dimension. The mass fractal dimension is a way of quantifying aggregate structure with $1 < d_F < 3$ (Chakraborti et al., 2003). Small fractal dimension values indicate very extended and tenuous structures while larger values indicate structures mechanically stronger and quite dense (Bushell, 2005).

$$R_{ci} = r_0\left(\frac{N}{k_c}\right)^{1/d_F} \tag{6}$$

2.4. Fragmentation rate

The fragmentation rate, S_i, can be given by the semi-empirical relation proposed by Kusters et al. (1997) (Eq. (7)). In Eq. (7), ε_{bi} corresponds to the critical energy dissipation rate that causes break-up of flocs.

$$S_i = \left(\frac{4}{15\pi}\right)^{1/2}\left(\frac{\varepsilon}{\nu}\right)^{1/2}\exp\left(\frac{-\varepsilon_{bi}}{\varepsilon}\right) \tag{7}$$

The critical energy dissipation rate can be related with the aggregate size using the relation observed experimentally by François (1987) (Eq. (8)). Eq. (8) shows that the energy dissipation necessary for breakage to occur is smaller for larger aggregates and, thus, larger flocs break up more easily. Moreover, the fragmentation rate increases as the shear rate ($G = (\varepsilon/\nu)^{0.5}$) increases.

$$\varepsilon_{bi} = \frac{B}{R_{ci}} \tag{8}$$

B is a fitting parameter which allows to define at which size class i the flocs start to break up and with what intensity breakage occurs in this size class i for a given shear rate.

2.5. Breakage distribution function

There are many ways to define the breakage distribution function. In this study, the binary breakage distribution function is used since it is simple to implement and it gives good results (Spicer and Pratsinis, 1996). In this case, we assume that the floc is divided into two flocs of the same size as described by Eq. (9) where V_0 is the volume of the primary particle.

$$\Gamma_{ij} = \frac{V_j}{V_i} \quad \text{for } j = i+1$$

$$\Gamma_{ij} = 0 \quad \text{for } j \neq i+1 \quad \text{where } \begin{matrix} V_i = 2^{i-1}V_0 \\ V_j = 2^iV_0 \end{matrix} \tag{9}$$

2.6. Flocs restructuring

When restructuring of flocs occurs, the fractal dimension that quantifies the flocs structure varies with the flocculation time. Hence, the model proposed by Bonanomi et al. (2004) and described by Eq. (10), was introduced into the population balance model, in Eq. (6), to take into account the decrease in the flocs size due to polymer reconformation.

$$\frac{dd_F}{dt} = \gamma(d_{F,max} - d_F) \tag{10}$$

In Eq. (10), γ is a fitting parameter and $d_{F,max}$ is the maximum fractal dimension value. Fractal dimension values are normally obtained experimentally by using techniques as microscopy or light scattering. The mass fractal dimension provides a mean of expressing the degree to which primary particles fill the space within the nominal volume occupied by an aggregate: for solid nonporous particles $d_F = 3$ and for porous particles $1 < d_F < 3$ (Liao et al., 2005). In addition, when aggregate restructuring occurs, the aggregate structure is no longer fractal because the applicability of the Rayleigh–Gans–Debye theory is limited. Restructuring takes place at large length scales and information about flocs structure is provided by the so called scattering exponent, *SE*, that is also determined from the scattering pattern (Liao et al., 2005). So, when light scattering techniques are used and when aggregate restructuring occurs, as is typical of flocculation by bridging, the flocs structure is better described by the scattering exponent, *SE* (Lin et al., 1990; Selomulya et al., 2002) and thus, in Eq. (10) as well as in Eq. (6), the mass fractal dimension, d_F, is replaced by the scattering exponent, *SE*.

In the second part of this study, since the decrease of the flocs size during the flocculation process is not only due to the flocs restructuring but also to the polymer degradation, we have implemented the equation proposed by Heath and co-workers in their first study (2003). Hence, the breakage irreversibility was introduced into the model by making the particle collision efficiency term decrease during flocculation time by using Eq. (11). In Eq. (11), C is the initial collision efficiency and D is a parameter for the rate of decrease in the collision efficiency with time. C and D are fitted parameters and should probably depend on other variables like polymer concentration or polymer characteristics.

$$\alpha = Ce^{-t/D} \tag{11}$$

2.7. Flocs size determination

Flocculation kinetics is normally analysed from the variation of the mean flocs size with flocculation time. Thus, in the population balance equation of the model (Eq. (1)) which describes the evolution of the number of particles in each size class with time, it

is necessary to transform the aggregate number concentration in each size class i to a scale of size. In this study, the volume mean size, $d[4,3]$ was calculated from the aggregate number distribution using equation below.

$$d[4,3] = \frac{\sum N_i D_i^4}{\sum N_i D_i^3} \tag{12}$$

In Eq. (12), N_i is the number of flocs in class i and D_i is the characteristic diameter of the class i and is calculated from Eq. (13). In Eq. (13), d_0 is the characteristic diameter for the class $i=1$ corresponding to the smallest size of the primary particles used in this work.

$$D_i = \left(2^{\frac{i-1}{d_F}}\right) d_0 \tag{13}$$

2.8. Solution of the model equations

The model proposed was solved numerically using the Runge–Kutta ordinary differential equation solver in Matlab®. The maximum number of intervals used was 30 ($i_{max}=30$) to guarantee that all the aggregates' sizes are present. The initial particle diameter was set to 0.1 μm which is the smallest size of the primary PCC particles. The shear rate (G) was constant and equals to 312 s^{-1} whereas the scattering exponent (SE) at time $t=0$ was assumed to be equal to 1.65. The shear rate (G) in the Mastersizer 2000 beaker was determined by CFD modelling using the COMSOL Multiphysics® software (Bouanini et al., 2006). In fact, because the shape of the shaft is very different from the common ones, it is necessary to make use of a CFD description of the flow in the beaker. Based on that description, we assumed the shear rate that describes the flow in the equipment beaker as the average shear rate. In fact, the velocity field of the fluid in the beaker, obtained with COMSOL Multiphysics®, for the stirring speed used, showed that the magnitude of the shear rate only differs in a small region very close to the stirrer baffles, being approximately constant in all the remaining region. The initial number concentration of the particles for the model (N for $t=0$) corresponds to the number particle size distribution obtained from the transformation of the volume distribution, acquired by the Mastersizer 2000, to a number distribution. The maximum scattering exponent comes, in each case, from the experimental data for $t=t_{max}$ (Antunes et al., 2008). In order to obtain a simulation curve as close as possible to the experimental curve, the parameters (α_{max}, B, γ) estimation was done by minimising the sum of squares errors between the model and the experimental results for the change in the volume mean diameter. The objective function used for parameter estimation is described by Eq. (14), which was implemented in the Matlab® simulation using the "fminsearch" function (Nelder–Mead Method).

$$\min_{\alpha_{max},B,\gamma} \psi = \sum_{t=0}^{t=t_{max}} (d[4,3]_{expt} - d[4,3]_{model})^2 \tag{14}$$

The experimental data used in this study refer to flocculation studies of PCC induced by C-PAMs of very high molecular weight and medium charge density. Three new C-PAM emulsions, developed and supplied by AQUA+TECH, were used in this study: Alpine-Floc™ E1 with a linear structure, Alpine-Floc™ E1+ with a low branched structure and Alpine-Floc™ E1++++ with a highly branched structure. The laser diffraction spectroscopy technique (LDS) was used to monitor the flocculation process giving, at each flocculation time, the volumetric flocs size distribution and the flocs structure (SE). The strategy used to monitor the flocculation process and the flocculation results are well described and discussed in a previous study (Antunes et al., 2008).

Additionally, the total solid volume was calculated for each flocculation time to ensure that the mass is not lost during the simulation. Calculations stop if the loss of volume is higher than 1%.

3. Results and discussion

For each experiment presented in Fig. 1, the proposed population balance model was applied. The outputs from the model are the optimized fitting parameters' values, the mean flocs size evolution, the scattering exponent evolution (presented in Fig. 2) and, for each flocculation time, the number flocs size distribution. The simulation time for the model with three fitting parameters is on an average 12 h.

The optimized fitting parameters that have originated the modelled results of Figs. 1–3 are summarized in Table 1. In order to quantify the degree of the model fit to the experimental results, a "goodness of fit" was calculated (Biggs and Lant, 2002) from equation below.

$$GoF = \frac{\overline{d[4,3]}_{expt} - st_{error}}{\overline{d[4,3]}_{expt}} \tag{15}$$

In Eq. (15), st_{error} is the standard error calculated from Eq. (16) where n is the number of measured points. In Eq. (16), st_{error} is divided by $n-3$ that corresponds to the number of degrees of freedom when fitting three model parameters.

$$st_{error} = \sqrt{\frac{\sum_{t=0}^{t=t_{final}} (d[4,3]_{expt} - d[4,3]_{model})^2}{n-3}} \tag{16}$$

When the "goodness of fit" is calculated in this manner, it is normally considered that for values higher than 90% the model offers a good approximation. Since in our case all the values of the "goodness of fit" obtained are above 90%, it is confirmed that the proposed model can be used to predict flocculation of such flocculation systems where bridging is the main mechanism.

In Fig. 2, the experimental variation of the scattering exponent is compared with the scattering exponent variation calculated from Eq. (10) for the three flocculants and for three different flocculant concentrations. In general, the modelled scattering exponent variations describe quite well the experimental flocs structure variations, allowing, in this manner, to obtain the flocculation kinetic profiles of Fig. 1. In Fig. 1, the experimental flocculation kinetics are compared with the modelled flocculation kinetics for the three flocculants and for each flocculant three concentrations have been studied. The intermediate flocculant dosage corresponds to the maximum flocculation found by the LDS technique (Antunes et al., 2008). For this optimum flocculant dosage, flocculation rate is faster and the flocs produced are larger.

The model selected, using three fitting parameters, is capable of simulating the same flocculation trends observed experimentally, i.e., the flocs size reaches rapidly a maximum and then starts to decrease due to flocs restructuring. Hence, these results demonstrated that for these flocculation systems the flocs structure information cannot be neglected.

The number size distributions obtained directly from the model have been converted to volume size distributions (Eq. (12)), since the LDS technique gives the size distribution based on volume. In Fig. 3, some examples of the flocs size distributions obtained from the model, for the E1++++ flocculant, are represented for 90 s and 14 min of flocculation time and are compared with the respective experimental data. The modelled results show that the modelled particle size distribution appears for the same size range as the experimental distributions, the same trends being observed, i.e., flocs size decreases during flocculation after reaching a maximum size in the kinetic curve

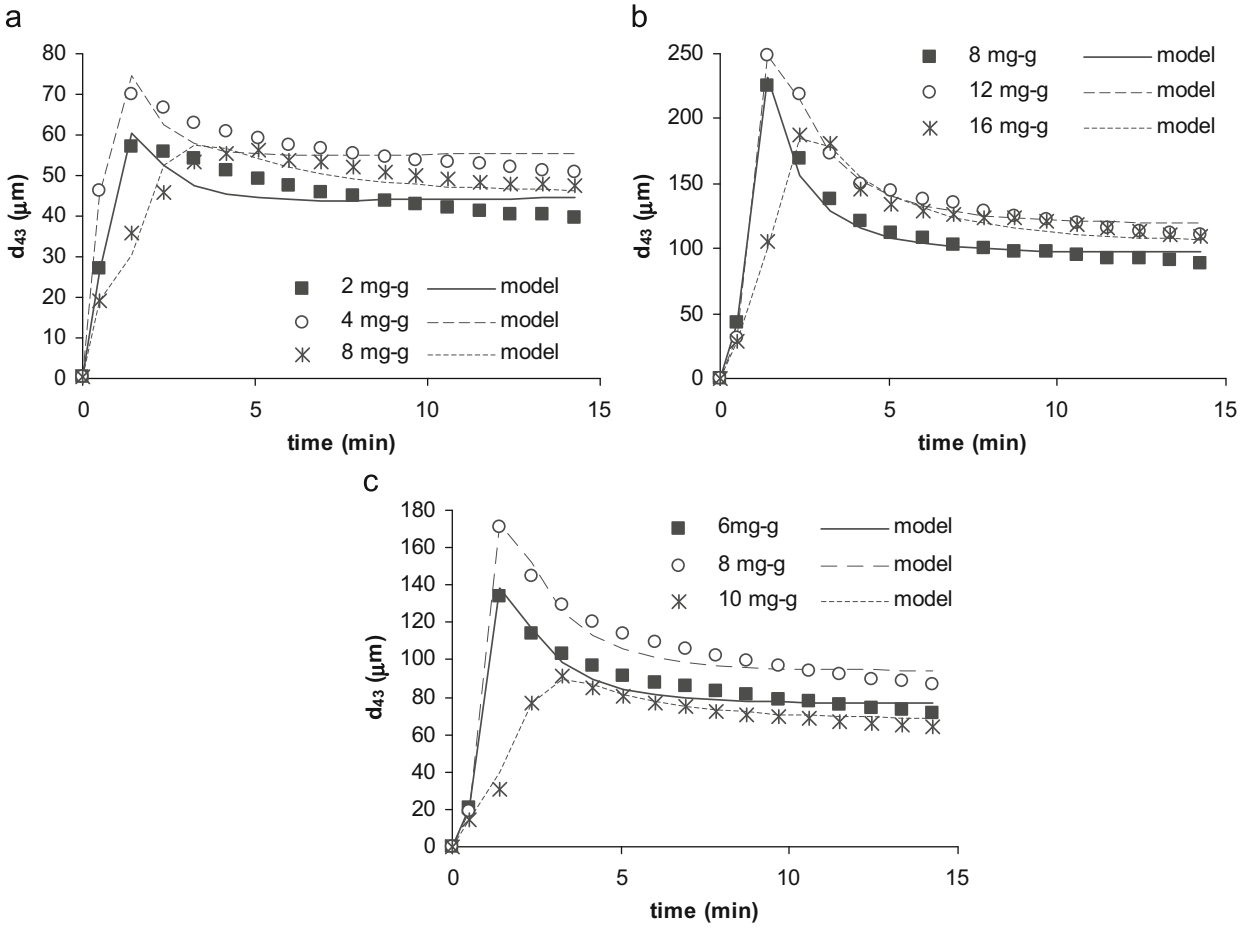

Fig. 1. Experimental and modelled flocculation kinetics for different flocculants type and flocculant concentrations: (a) E1, (b) E1+ and (c) E1++++.

(from 90 s to 14 min), due to flocs restructuring. Nevertheless, some deviations are clear between the modelled and the experimental distributions, mainly due to the wider nature of the experimental particle size distribution. This must be due to limitations of the numerical methodology, namely as far as the number and width of the size classes selected, dictated by the computational limitations. It is also apparent from Fig. 2 that the larger deviations in the *SE* profiles are observed for the higher flocculant concentrations, mainly in the case of E1+. This can be associated with the uncertainty of the experimental values which increase as polymer concentration increases due to equipment limitations, mainly as a consequence of adhesion problems.

The values of the fitting parameters of Table 1 were then correlated with the polymer properties and polymer concentration. Fig. 4 represents the values of the parameters α and γ as a function of polymer concentration for the three polymers studied.

Fig. 4 shows that an increase in the maximum collision efficiency factor (α_{max}) corresponds always to an increase of the kinetic parameter for flocs restructuring (γ). This indicates that the faster the flocculation kinetics is, the faster the flocs restructuring rate will be. Since flocculation kinetics becomes slower as the flocculation concentration above the optimum dosage increases (Fig. 1 and Antunes et al., 2008) it was expected that these two parameters would decrease with the flocculant dosage increase, as can be observed in Fig. 4. In fact, the flocculation kinetics becomes slower as the flocculant dosage increases because there is a higher competition between polymer chains. On the other hand, it becomes also more difficult for the adsorbed polymer chains to re-conform which results in a slower restructuring rate (Antunes et al., 2008).

Figs. 5 and 6 represent the three fitting parameters (α_{max}, γ and B) as a function of flocs sizes and degree of restructuring, respectively, for the three polymers studied and for the optimum flocculant concentration of each polymer. The optimum flocculant dosage corresponds to the intermediate flocculant concentration modelled. The degree of restructuring was calculated as the ratio of the difference between the flocs size at the maximum and at the end of the flocculation kinetic curve and the flocs size corresponding to the maximum size in the same curve (reorganization percentage).

Fig. 5 shows that the maximum collision efficiency factor and the kinetic parameter for flocs restructuring are higher for the linear polymer (E1). Indeed, as seen in a previous paper (Antunes et al., 2008), flocculation kinetics and flocs restructuring rate are the fastest for the linear polymer. The flocs size produced with E1 stabilizes earlier. Hence, the branched polymer structure impairs the velocity of the flocculation process.

Moreover, the parameter related with fragmentation rate, B, increases with the increase of the flocs size. This was expected since, as the parameter B increases, flocs break up occurs for higher size classes. In fact, larger flocs are more susceptible to breakage. Furthermore, an increase in the parameter B corresponds to a decrease in the other parameters. Thus, larger flocs are obtained at a lower flocculation rate and lower restructuring rate (more open flocs). This agrees with the fitting parameters variation with the degree of flocs restructuring (Fig. 6). In Fig. 6, reorganization refers to the degree of flocs restructuring as defined above. Again, flocs restructuring is more notorious when the reconformation of the polymer chains on the particle surface is more difficult. Thus, the flocs take longer to reach the final,

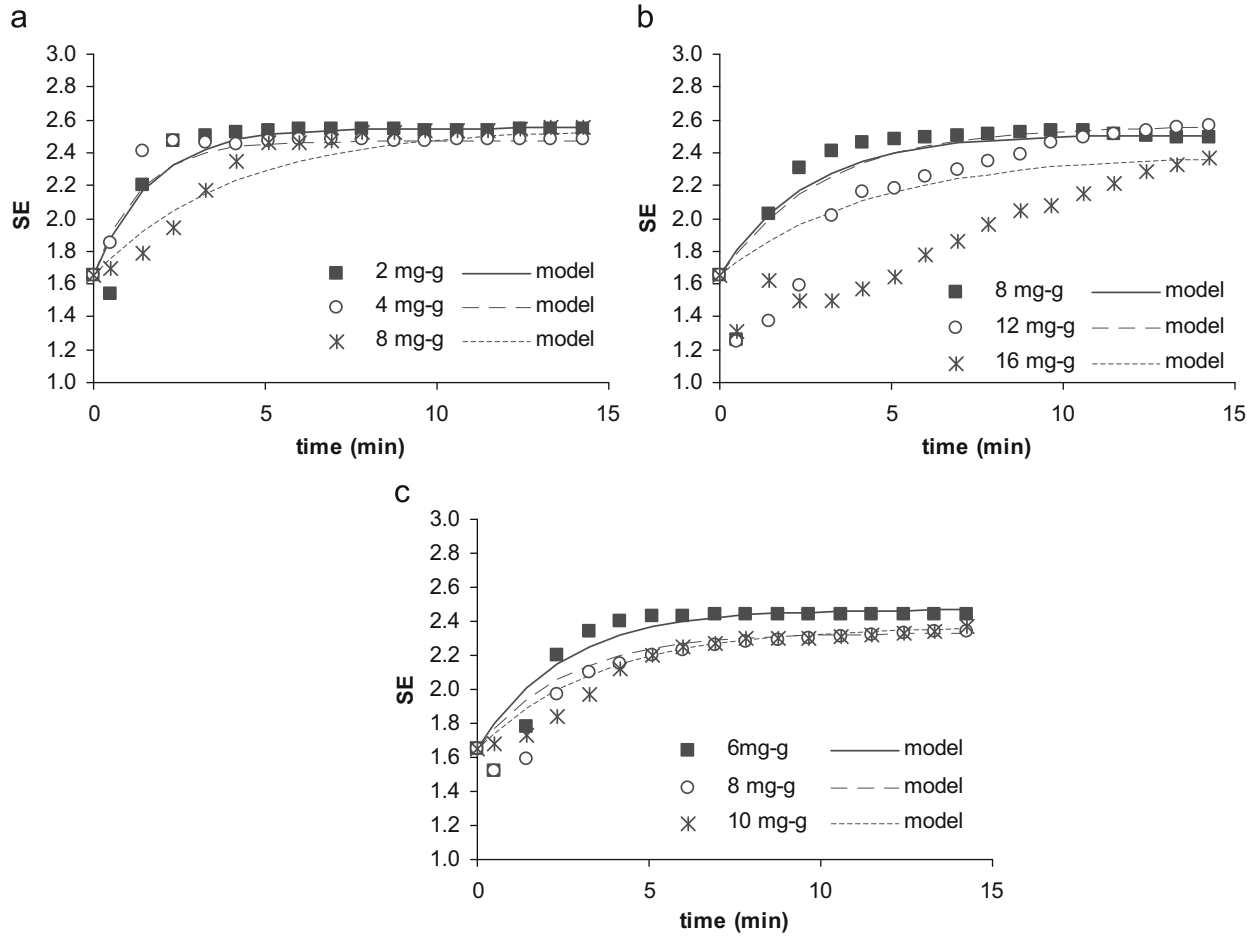

Fig. 2. Experimental and modelled structure variation for different flocculants type and flocculant concentrations: (a) E1, (b) E1+ and (c) E1++++.

Table 1
Optimum fitting parameters for E1, E1+ and E1++++ (three parameters model).

Flocculant dosage (mg/g)		α_{max}	B	γ	GoF[a] (%)
E1	2	0.890	17.8	0.602	91
	4	0.983	19.8	0.760	93
	8	0.360	21.2	0.248	92
E1+	8	0.524	38.7	0.402	94
	12	0.416	51.7	0.336	96
	16	0.262	40.2	0.231	95
E1++++	6	0.525	29.7	0.408	94
	8	0.433	31.4	0.395	94
	10	0.312	26.1	0.281	95

[a] *GoF*—"Goodness of fit".

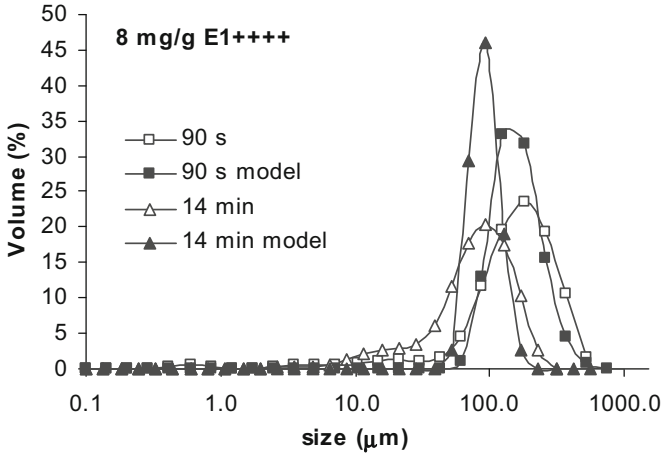

Fig. 3. Flocs size distributions from experimental and model results for 8 mg of E1++++/g of PCC.

stable configuration and restructuring is more visible because it occurs more slowly. The branched polymer structure impairs again the flocculation process.

From the plot in Fig. 7, it is possible to observe that an increase in the parameter B corresponds to a decrease of the scattering exponent at the maximum in the kinetics, i.e., in this case the flocs structure is more open in the beginning of the flocculation process, as expected. This agrees with the fact that B increases as the flocs size increases. Indeed, it was shown in a previous study (Antunes et al., 2008) that larger flocs exhibit a more open structure.

Furthermore, it is known that the radius of gyration, R_g, is influenced by the number of polymer branches. In fact, for a constant molecular weight, as the number of branches increase, the polymer radius of gyration must decrease (Huang et al., 2000). It was then expected that as R_g decreases both the restructuring and the flocculation rates decrease. This is confirmed by Fig. 8 where the fitting parameters are presented as a function of the polymer number of branches, the variation observed in these parameters following the trend expected for R_g. Indeed, the

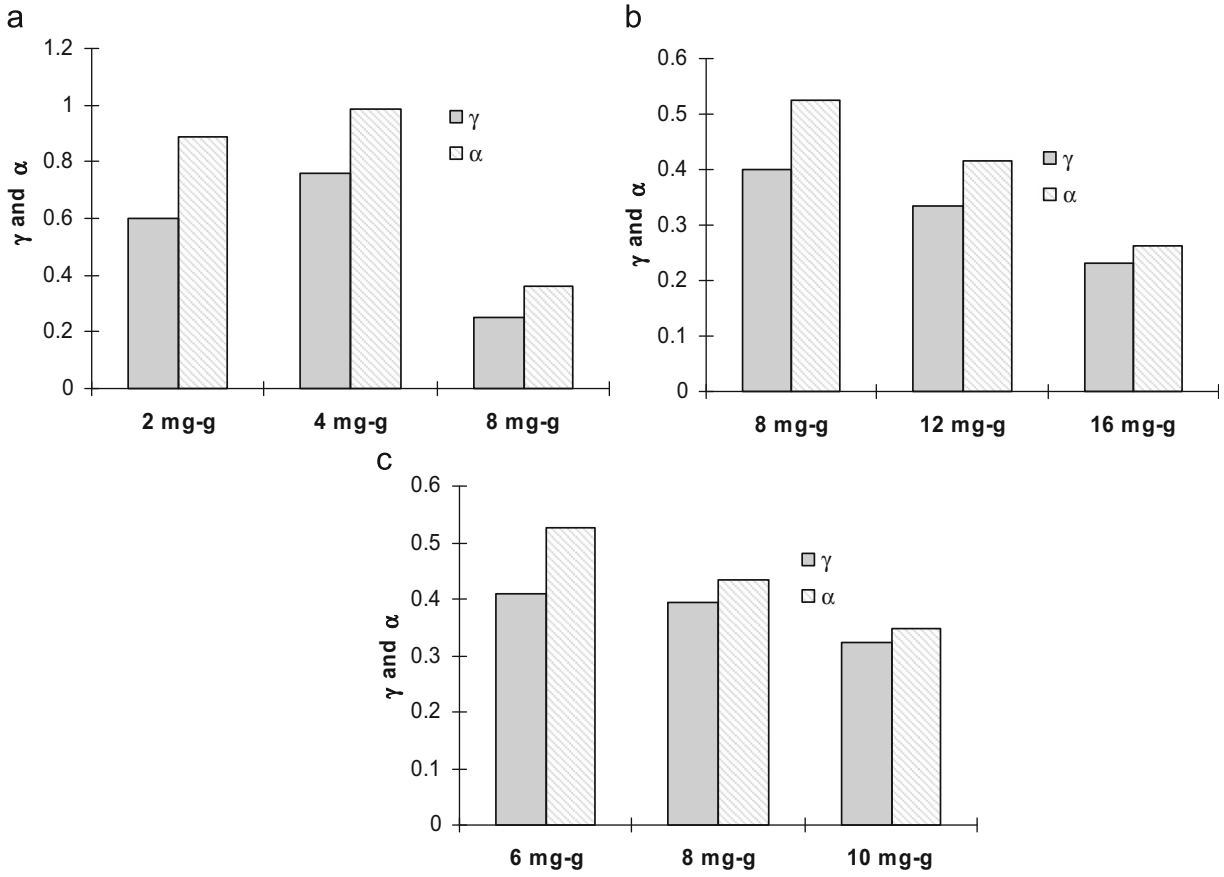

Fig. 4. α_{max} and γ as a function of flocculant concentration for (a) E1, (b) E1+ and (c) E1++++.

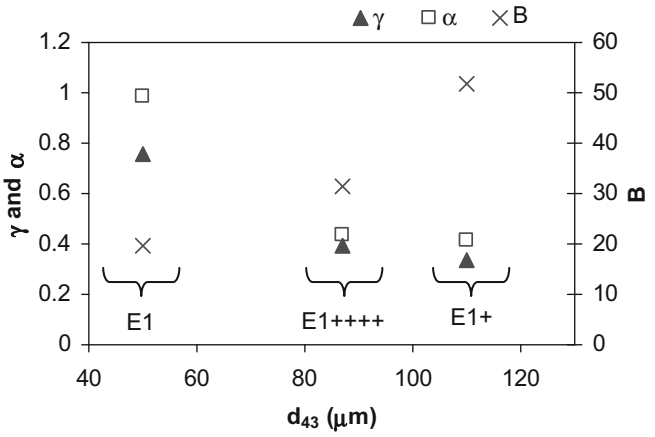

Fig. 5. Fitting parameters as a function of the mean flocs size at $t=14$ min and for the optimum flocculant dosage.

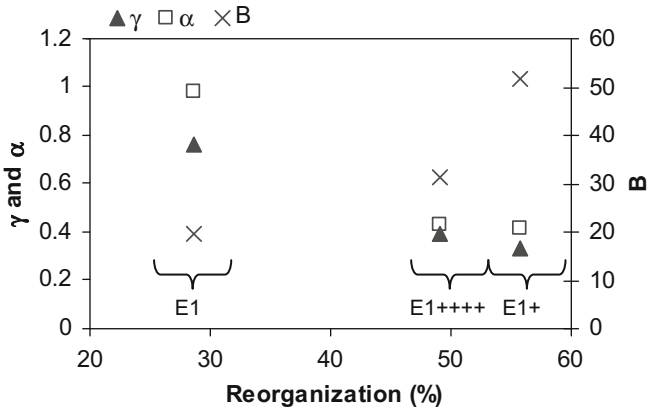

Fig. 6. Fitting parameters as a function of the degree of flocs restructuring for the optimum flocculant dosage.

polymer layer thickness at the particles surface must decrease due to the reduction of the polymer radius of gyration. Consequently, collision between particles becomes more difficult. On the other hand, the conformation that the polymer adopts when branches exist makes the polymer reconformation at the particles surface more difficult as referred previously and, thus, lower values for γ are obtained.

In addition to the study already presented, the decrease of the collision efficiency factor, given by Eq. (11), was also implemented in the model. This methodology enables accounting for the decrease on the flocs size during flocculation due to polymer degradation. In this case, the model has four fitting parameters: the parameter related with the fragmentation rate (B), the kinetic parameter of restructuring rate (γ), the maximum collision efficiency factor at $t=0$ (C) and the parameter for the rate of decrease in the collision efficiency (D).

Simulations were only performed for the E1 and E1++++ polymers. Table 2 summarises the optimum fitting parameters obtained for the experiments modelled. Comparing with the results of Table 1, it is possible to conclude that the small improvement of adjustment between experimental and calculated data does not justify using this more elaborated model to simulate the flocculation process, for the systems studied. In fact, in all tests, the "goodness of fit" just slightly increases if the decrease of the collision efficiency factor during

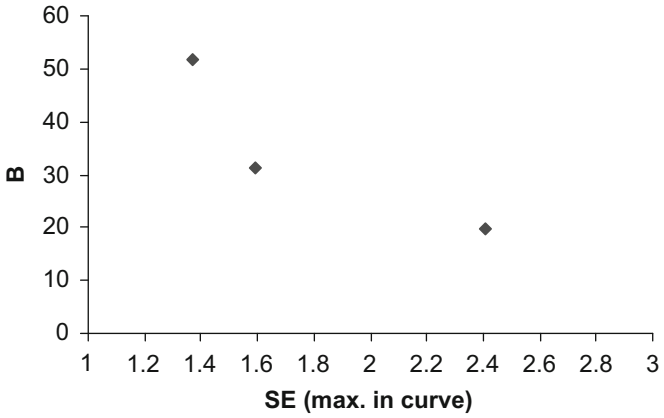

Fig. 7. Fitting parameter B as a function of the scattering exponent at the maximum in the kinetic curve for the optimum flocculant dosage for the three polymers.

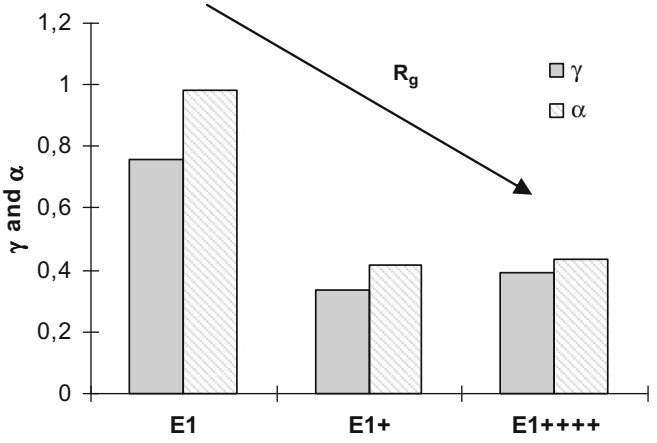

Fig. 8. α_{max} and γ as a function of polymer branching and R_g for the optimum flocculant dosage.

Table 2
Optimum fitting parameters for E1 and E1++++ (four parameters model).

Flocculant dosage (mg/g)		C	B	γ	D	GoF[a] (%)
E1	2	0.881	19.8	0.622	12.8	93
	4	1.07	21.3	0.776	17.1	96
	8	0.636	22.1	0.244	43.4	92
E1++++	6	0.455	31.4	0.427	25.3	96
	8	0.978	31.8	0.394	97.3	98
	10	0.331	26.0	0.280	91.2	96

[a] *GoF*—"Goodness of fit".

flocculation is considered. The difference between the computational time to perform simulations with three and four parameters is also a reason not to have proceeded further with this last model. For one more parameter, the simulation time was multiplied by a factor of more than four.

It is, nevertheless, interesting to plot the maximum collision efficiency factor decrease during the flocculation process (Fig. 9). Indeed, the collision efficiency factor slightly decreases for the higher flocculant dosage indicating that polymer degradation is insignificant, but also that an excess of flocculant allows producing stronger flocs as verified by Blanco et al. (2005) and by Rasteiro et al. (2008a). When comparing the two flocculants, the decrease of the collision efficiency factor is much more notorious for the linear polymer. This indicates that the polymer degradation is more important for flocs produced with the linear polymer. As seen before, for the linear polymer the restructuring rate is faster and, thus, the flocs size reaches quickly a steady-state. Consequently, the decrease of the flocs size during flocculation is mainly due to flocs break up, which leads to polymer degradation, while, for the branched polymer, the decrease is mainly due to flocs restructuring (collision efficiency remains almost constant).

4. Conclusions

Flocculation of precipitated calcium carbonate with C-PAMs of very high molecular weight and medium charge density was successfully described using a population balance model proposed by Hounslow et al. (1988) and Spicer and Pratsinis (1996) where, additionally, the flocs restructuring was taken into account. It was demonstrated that for the flocculation system presented in this work, where bridging is the dominating mechanism, the flocs structure information cannot be neglected.

The fitting parameters correlate well with the effect of the flocculant concentration and the degree of polymer branching on flocculation kinetics and on flocs characteristics (size and structure).

The possibility of using a model with four parameters, taking into account the decrease of collision efficiency with time, was abandoned since only minor improvements in the fitting were obtained while the computation time increased dramatically.

The model proposed allows one not only to predict in advance the flocs characteristics (size and structure) and the flocculation kinetics for a given process, but it will also allow us to chose operating conditions and the flocculant that originate aggregates with given properties and, consequently, a given performance. In the case of the papermaking process, this feature of the model is of great importance to define the conditions that will lead to an adequate balance between retention, drainage and formation, which depend on flocs size and structure.

For future work, it will be interesting to further develop the model in order to consider also, in a quantitative way, the influence of the polymer concentration and of the polymer structure since they are the main parameters affecting the flocculation performance.

Notation

B	fitting parameter for fragmentation rate
C	collision efficiency factor for $t=0$
d_F	mass fractal dimension
$d_{F,max}$	maximum mass fractal dimension
$d[4,3]$	volume mean size, μm
D	fitting parameter for $d\alpha/dt$
D_i	characteristic diameter of the class i, cm
G	average shear rate, s^{-1}
k_c	constant ≈ 1
k_B	Boltzmann constant, J/K
n	number of measured points
N	number of primary particles in an aggregate
N_i	number concentration of flocs containing 2^{i-1} particles, $\#/cm^3$
r_0	primary particle radius, cm
R_c	effective capture radius, cm
R_g	radius of gyration, nm
st_{error}	standard error
SE	scattering exponent

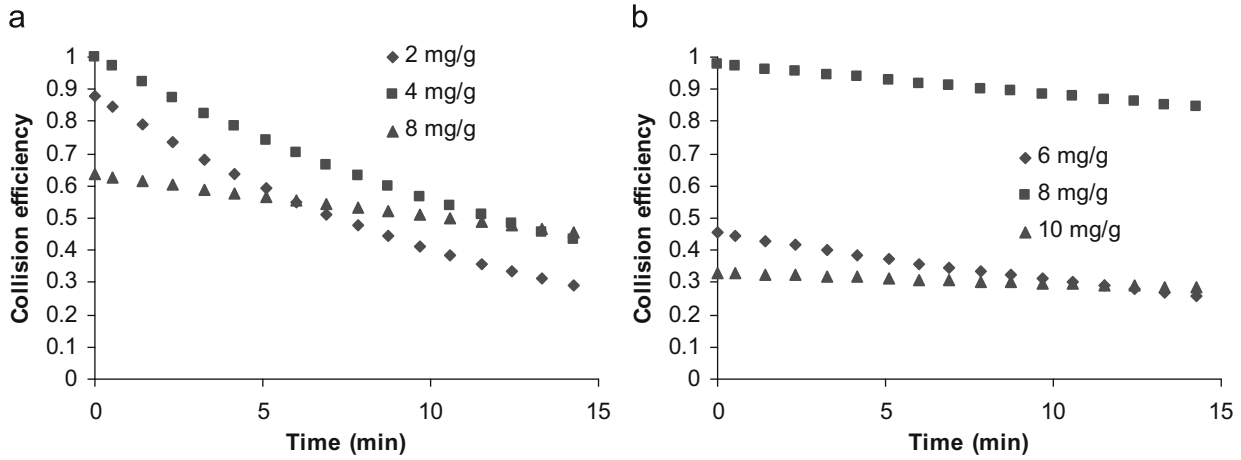

Fig. 9. Variation of the calculated maximum collision efficiency factor with flocculation time for (a) E1 and (b) E1+++ (four parameters model).

S_i fragmentation rate of flocs in the ith interval, s^{-1}
t time, s
T absolute temperature, K
v_i volume of flocs in the ith interval
V_0 volume of primary particle, cm^3
x,y fitting parameters for α_{ij}

Greek letters

α_{ij} collision efficiency between aggregates in the ith and jth intervals
α_{max} maximum collision efficiency
β_{ij} collision frequency between aggregates in the ith and jth intervals, cm^3/s
γ fitting parameter for dd_F/dt
Γ_{ij} breakage distribution function
ε average energy dissipation rate, m^2/s^3
ε_{bi} critical energy dissipation rate, m^2/s^3
μ fluid viscosity, Pa s
ν fluid kinematic viscosity, m^2/s

Acknowledgements

The authors thank the FCT (Fundação para a Ciência e Tecnologia, Portugal) for financial support and AQUA+TECH Specialties SA (La Plaine, Geneva, Switzerland) for supplying the flocculant samples.

References

Adler, P.M., 1981a. Streamlines in and around porous particles. Journal of Colloid and Interface Science 81, 531–535.
Adler, P.M., 1981b. Heterocoagulation in shear flow. Journal of Colloid and Interface Science 83, 106–115.
Antunes, E., Garcia, F.A.P., Ferreira, P., Blanco, A., Negro, C., Rasteiro, M.G., 2008. Effect of water cationic content on flocculation, flocs resistance and reflocculation capacity of PCC induced by polyelectrolytes. Industrial and Engineering Chemistry Research 47, 6006–6013.
Biggs, C.A., Lant, P.A., 2002. Modelling activated sludge flocculation using population balances. Powder Technology 124, 201–211.
Biggs, S., Habgood, M., Jameson, G.J., Yan, Y.D., 2000. Aggregate structures formed via a bridging flocculation mechanism. Chemical Engineering Journal 80, 13–22.
Blanco, A., Negro, C., Fuente, E., Tijero, J., 2005. Effect of shearing forces and flocculant overdose on filler flocculation mechanisms and flocs properties. Industrial and Engineering Chemistry Research 44, 9105–9112.
Bonanomi, E., Morari, M., Sefcik, J., Morbidelli, M., 2004. Analysis and control of turbulent coagulator. Industrial and Engineering Chemistry Research 43, 6112–6124.
Bouanini, M., Bascoul, A., Mouret, M., Sellier, A., 2006. Hydrodynamic simulation of non Newtonian fluid in an agitated vessel. In: Proceedings of the Comsol Users Conference, Paris.
Bushell, G., 2005. Forward light scattering to characterise structure of flocs composed of large particles. Chemical Engineering Journal 111, 145–149.
Chakraborti, R.K., Gardner, K., Atkinson, J., Van Benschoten, J., 2003. Changes in fractal dimension during aggregation. Water Research 37, 873–883.
Flesch, J.C., Spicer, P.T., Pratsinis, S.E., 1999. Laminar and turbulent shear-induced flocculation of fractal aggregates. A.I.Ch.E. Journal 45, 1114–1124.
François, R.J., 1987. Strength of aluminium hydroxide flocs. Water Research 21 (9), 1023–1030.
Han, M.Y., Lawler, D.F., 1992. The (relative) insignificance of G in flocculation. Journal of American Water Works Association 84, 79–91.
Heath, A.R., Bahri, P.A., Fawell, P.D., Farrow, J.B., 2006. Polymer flocculation of calcite: population balance model. A.I.Ch.E. Journal 52 (5), 1641–1653.
Heath, A.R., Koh, P.T.L., 2003. Combined population balance and CFD modelling of particle aggregation by polymeric flocculant. In: Third International Conference on CFD in the Minerals and Process Industries, Melbourne, Australia.
Hounslow, M.J., Ryall, R.L., Marshall, V.R., 1988. A discretized population balance for nucleation, growth and aggregation. A.I.Ch.E. Journal 34, 1821–1832.
Huang, Y., Bu, L.W., Zhang, D.Z., SU, C.W., Xu, Z.D., Bu, L.J., Mays, J.W., 2000. Characterization of star-block copolymers having PS-b-PI arms via SEC/RT/RALLS/DV. Polymer Bulletin 44, 301–307.
Kusters, K.A., Wijers, J.G., Thoenes, D., 1991. Numerical particle tracking in a turbine agitated vessel. In: Proceedings of the Seventh European Conference on Mixing, vol. II, Brugge, Belgium, pp. 429–441.
Kusters, K.A., Wijers, J.G., Thoenes, D., 1997. Aggregation kinetics of small particles in agitated vessels. Chemical Engineering Science 52, 107–121.
Liao, J.Y.H., Selomulya, C., Bushell, G., Bickert, G., Amal, R., 2005. On different approaches to estimate the mass fractal dimension of coal aggregates. Particle and Particle Systems Characterization 22, 299–309.
Lin, M.Y., Klein, R., Lindsay, H.M., Weitz, D.A., Ball, R.C., Meakin, P., 1990. The structure of fractal colloidal aggregates of finite extent. Journal of Colloid and Interface Science 137, 263–280.
Norell, M., Johansson, K., Persson, M., 1999. Retention and drainage. In: Neimo, L. (Ed.), Book 4: Papermaking Chemistry, Papermaking Science and Technology. Tappi Press, Finland.
Rasteiro, M.G., Garcia, F.A.P., Ferreira, P., Blanco, A., Negro, C., Antunes, E., 2008a. The use of LDS as a tool to evaluate flocculation mechanisms. Chemical Engineering and Processing 47, 1329–1338.
Rasteiro, M.G., Garcia, F.A.P., Ferreira, P., Blanco, A., Negro, C., Antunes, E., 2008b. Evaluation of flocs resistance and reflocculation capacity using the LDS technique. Powder Technology 183, 231–238.
Saffman, P.G., Turner, J.S., 1956. On the collision of drops in turbulent clouds. Journal of Fluid Mechanics 1 (16), 16–30.
Selomulya, C., Bushell, G., Amal, R., Waite, T.D., 2002. Aggregation mechanisms of latex of different particle sizes in a controlled shear environment. Langmuir 18, 1974–1984.
Selomulya, C., Bushell, G., Amal, R., Waite, T.D., 2003. Understanding the role of restructuring in flocculation: the application of a population balance model. Chemical Engineering Science 58, 327–338.
Serra, T., Casamitjana, X., 1998. Modelling the aggregation and break-up of fractal aggregates in a shear flow. Applied Scientific Research 59, 255–268.
Smoluchowski, M.V., 1917. Versuch einer mathematischen theorie der koagulationskinetic kolloider lösungen. Zeitschrift fur Physikalische Chemie 92, 124–168.
Soos, M., Sefcik, J., Morbidelli, M., 2006. Investigation of aggregation, breakage and restructuring kinetics of colloidal dispersions in turbulent flows by population balance modelling and static light scattering. Chemical Engineering Science 61, 2349–2363.
Spicer, P.T., Pratsinis, S.E., 1996. Coagulation and fragmentation: universal steady-state particle-size distribution. A.I.Ch.E. Journal 42 (6), 1612–1620.

Swerin, A., Ödberg, L., Wågberg, L., 1996. An extended model for the estimation of flocculation efficiency factors in multicomponent flocculant systems. Colloidal Surface 113, 25–38.
Swift, D.L., Friedlander, S.K., 1964. The coagulation of hydrosols by Brownian motion and laminar shear flow. Journal of Colloid and Interface Science 19, 621–647.
Thomas, D.N., Judd, S.J., Fawcett, N., 1999. Flocculation modelling: a review. Water Research 33 (7), 1579–1592.
Wu, R.M., Lee, D.J., 1998. Hydrodynamic drag force exerted on a moving floc and its implication to free-settling tests. Water Research 32, 760–768.
Yukselen, M.A., Gregory, J., 2004. The reversibility of floc breakage. International Journal of Mineral Processing 73, 251–259.